

We are IntechOpen, the world's leading publisher of Open Access books Built by scientists, for scientists

6,900

Open access books available

186,000

International authors and editors

200M

Downloads

Our authors are among the

154

Countries delivered to

TOP 1%

most cited scientists

12.2%

Contributors from top 500 universities



WEB OF SCIENCE™

Selection of our books indexed in the Book Citation Index
in Web of Science™ Core Collection (BKCI)

Interested in publishing with us?
Contact book.department@intechopen.com

Numbers displayed above are based on latest data collected.
For more information visit www.intechopen.com



Supramolecular Materials Based on Ionic Self-Assembly: Structure, Property, and Application

Jinglin Shen, Shiling Yuan and Xia Xin

Additional information is available at the end of the chapter

<http://dx.doi.org/10.5772/67906>

Abstract

The technique of ionic self-assembly (ISA), on the basis of electrostatic interactions, is a powerful tool to create new material nanostructures and chemical objects due to its advantages of facility, reliability, cost saving, flexibility, and universality. It has attracted great attention because of its promising applications in catalysis, drug delivery, and molecular detection. This review focuses on recent advances in the construction of self-assemblies with different morphologies on the basis of ISA strategy and its applications. The ISA method provides an opportunity to generate complex and hierarchical assemblies with tunable properties, which is regarded as a very promising case of supramolecular chemistry.

Keywords: ionic self-assembly, amphiphilic molecule, electrostatic interaction, supramolecular materials

1. Introduction

Supramolecular self-assembly, which makes use of molecules instead of atomic units, offers a bottom-up approach to the construction of new materials on multiple length scales without complex organic synthesis [1–10]. The driving forces for supramolecular chemistry are noncovalent interaction ranging from host-guest interaction [11], hydrogen bonding [12], van der Waals interaction [13], π – π stacking [14], electrostatic interactions [15] and hydrophobic effect [16]. **Table 1** summarizes most of this noncovalent interaction, as well as of its structure-determining properties [17]. Among them, the theme of ionic self-assembly (ISA) on the basis of electrostatic interactions was first described by Faul and Antonietti [17]. Different with the simple coulombic binding of salts, the ISA is usually accompanied by a cooperative binding (π – π stacking, hydrophobic effect, and van der Waals interaction) which propagates toward

the final self-assembly structures [17]. The ISA strategy is very easily available, reliable, and flexible and is much broader in application than multiple hydrogen bonding or stable metal coordination.

In this chapter, we provide an overview of work that contributed to establishing functional soft materials on the basis of ISA strategy and advancing the usefulness in the several areas such as soft matter template, luminescent materials, and inorganic-organic hybrid materials.

Type of interaction	Strength [kJ mol ⁻¹]	Range	Character
Van der Waals	51	Short	Non-selective, non-directional
H-bonding	5–65	Short	Selective, directional
Coordination binding	50–200	Short	Directional
“Fit interaction”	10–100	Short	Very selective
“Amphiphilic”	5–50	Short	Non-selective
Ionic	50–250 ^a	Long	Non-selective
Covalent	350	Short	Irreversible

^aDependent on solvent and ion solution; data are for organic media.

Table 1. Methods of self-assembly listed by invoked secondary interactions [17].

2. Dye-surfactant ISA materials

Dye molecules are almost the ideal building blocks for supramolecular chemistry, because they are easily available and have multiple functional groups, which possess a defined and regular shape (extended π system) and can facilitate mutual interactions, inducing them to have photoelectric functions and can form more complex structures, such as soft gels, liquid crystals, as well as plate-like and needle-like single crystals [18, 19]. Besides, the surfactant molecule plays a special role in surface chemistry. Especially, surface active ionic liquids (SAILs) such as imidazolium-, pyrrole-based ionic liquids have attracted widespread interest for their outstanding performance in biomaterials, photoelectricity, and environmentally friendly trades, since they possess good biocompatibility, low critical micellar concentrations, wide liquid range, and high thermal stability [20, 21]. Thus, the introduction of charged dye molecules or surfactants as ISA components will generate novel properties and structures of the systems and enrich the ranges and contents of ISA.

However, structures of supramolecular materials constructed by dye-surfactant have been limited to 1D and 2D structures, such as fiber and flake morphologies, and mostly have no fluorescent property, which greatly restricts the application of the material [22, 23]. For example, highly ordered fibers constructed by dyes and surfactants have been reported by Faul [24]. Zheng et al. also prepared highly ordered supramolecular microfibers through ISA strategy from complexes of the SAIL N-tetradecyl-N-methylpyrrolidinium bromide (C₁₄MPB) and anionic dye methyl orange (MO) with the aiding of patent blue VF sodium salt (PB) (**Figure 1a–g**) [23]. The crystal structure of microfibers can be indexed as a typical hexagonal columnar mesophase by XRD (**Figure 1h**). The driving force for the formation of microfiber

is hydrogen-bonding interactions, π - π stacking interactions, especially, the role of PB whose big disc-like structure favors the formation of a one-dimensional supramolecular material.

Based on the literature work, Xin and coworkers constructed giant vesicles (1–10 μm) via a facile ISA strategy using an anionic dye Acid Orange II (AO) and an oppositely charged ionic-liquid-type cationic surfactant 1-tetradecyl-3-methylimidazolium bromide ($\text{C}_{14}\text{mimBr}$) (**Figure 2a–c**) [25]. It is concluded that the electrostatic interaction, hydrophobic effect, and π - π stacking interaction play key roles in this self-assembly process. Importantly, the giant vesicles can act as a smart microcarrier to load and release carbon quantum dots (CQDs) under control (**Figure 2d, e**). Besides, the giant vesicles could also be applied as a microreactor to synthesize monodispersed Ag nanoparticles with diameter of about 5–10 nm which exhibited the ability to catalyze reduction of 4-nitroaniline (**Figure 2f, g**). Therefore, it is indicated that the AO/ $\text{C}_{14}\text{mimBr}$ assemblies hold promising applications in the areas of microencapsulation, catalyst support, and light weight composites owing to their huge sizes, and large microcavities.

Moreover, giant vesicle could also be prepared by anionic dye MO and an oppositely charged SAILs $\text{C}_{14}\text{mimBr}$ (**Figure 3a–d**) [26]. The giant vesicle performs fluorescence property owing to the break of π - π stacking of MO molecules (**Figure 3c**), and the formation of giant vesicle was confirmed by the fusion of small vesicle with the trace of TEM and DLS (**Figure 3d, i**). The

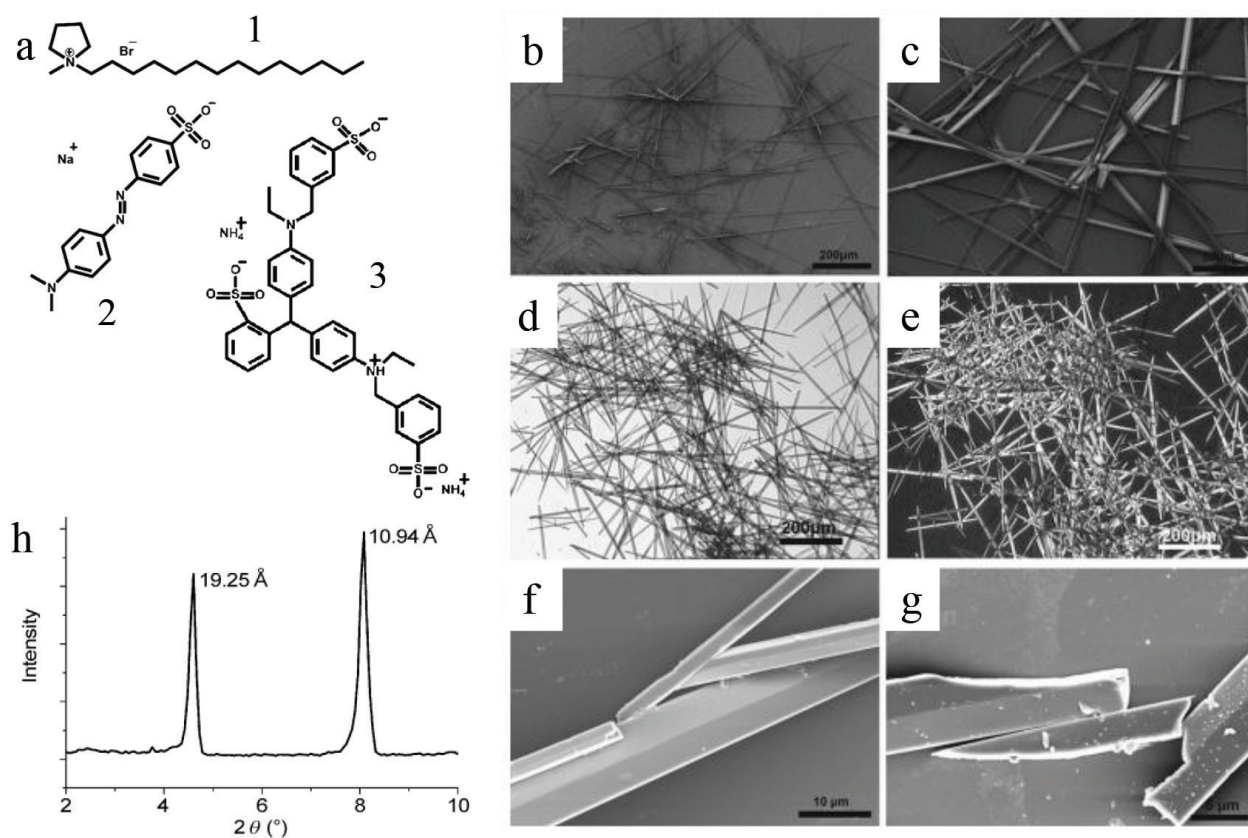


Figure 1. (a) Structures of the three components: (1) C_{14}MPB , (2) MO, and (3) PB. (b, c, f, g) SEM images (d) OM image and (e) POM image of the supramolecular microfibers. (h) XRD pattern of microfibers [23].

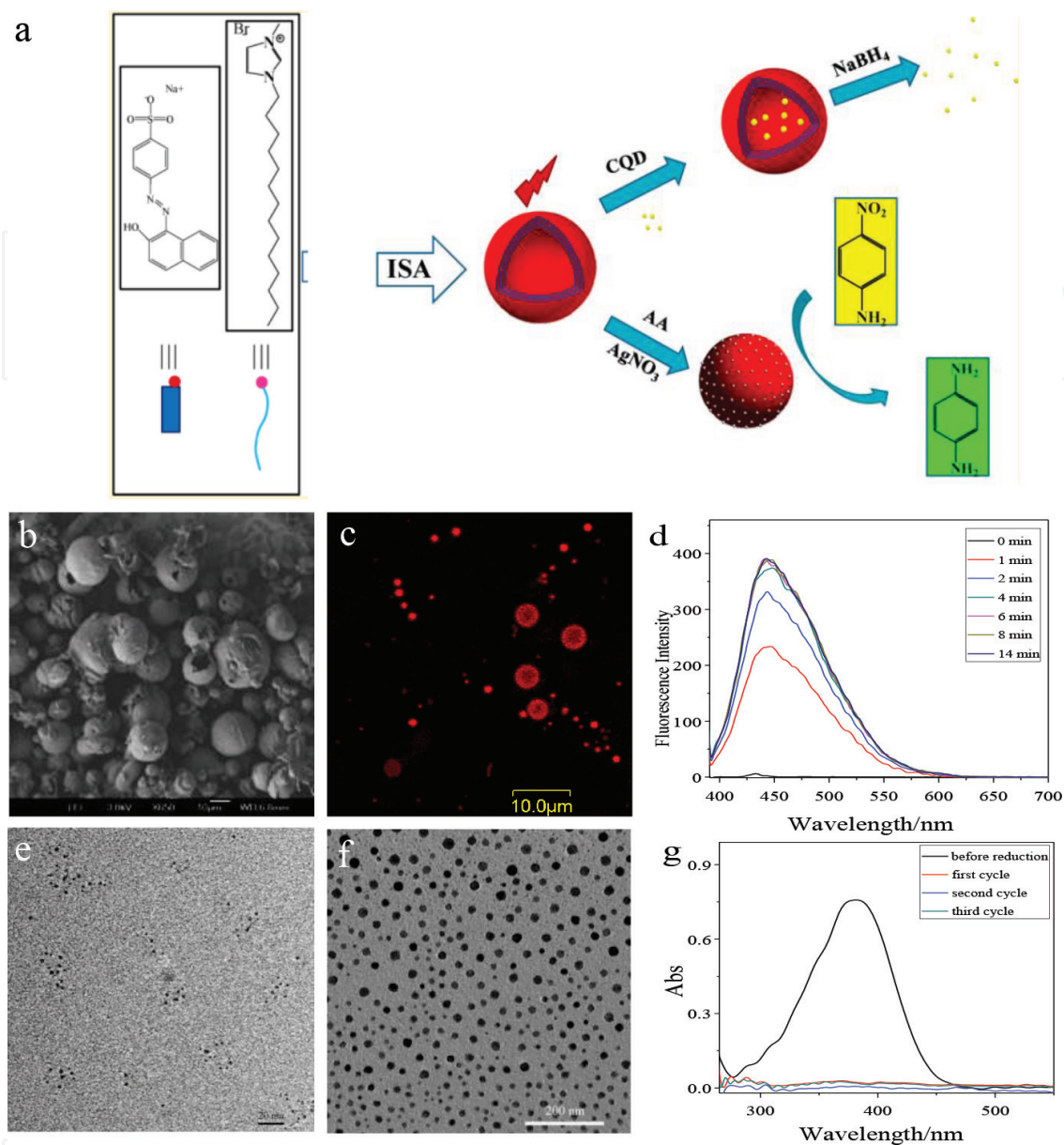


Figure 2. (a) Schematic demonstration of formation of giant vesicle and its applications for smart microcarrier and microreactor. (b) SEM and (c) CLSM images of giant vesicles formed by 0.5 mmol L^{-1} AO/ 0.5 mmol L^{-1} C₁₄mimBr. (d) Releasing of CQDs with the addition of NaBH₄. (e) TEM image of CQDs. (f) TEM image of Ag nanoparticle. (g) UV-vis spectra of 4-nitroaniline before and after reduction [25].

MO/C₁₄mimBr system also shows an interesting pH chromism phenomenon. Consequently, the MO/C₁₄mimBr system displays abundant aggregate morphologies with the changing of pH that complex fluorescent structures formed at pH > 4 and simple nonfluorescent structures formed at pH < 4 (**Figure 3e–h**). This is attributed to that MO moieties take a more conjugated coplanar state bridged by N=N under alkaline conditions, whereas MO takes a quinoid structure crossed by N–N resulting the break of conjugated configuration with the decreasing of pH (**Figure 3j, k**) [27]. Thus, the fluorescence behavior can be predicted with the color change directly visible to the naked eye by changing the pH. It is expected that the facile and innovative design of supramolecular material by the ISA strategy could be used as pH detection probes and microreactors.

Recently, one kind of biomolecule, bile salts, has been developed as building blocks for various functional nanomaterials [28, 29]. All of the bile salts possess a rigid, nearly planar hydrophobic steroid backbone and have polar hydroxyl groups on the concave α -face and methyl groups on the convex β -face [30, 31]. The ionic head with a carboxyl group is linked to the steroid ring through a short alkyl chain. Sodium deoxycholate (NaDC) is a bile salt and also an important biological surfactant which widely exists in the body of vertebrate [32]. The interesting structure of NaDC leads to novel and abundant self-assembly behavior in solution. For example, Xin and coworkers chose NaDC and a cationic dye (RhB) to construct soft materials [33]. In this system, different morphologies with high hierarchies can be reversibly controlled by varying the ratio of the two components (NaDC and RhB) and that the morphologies can switch between porous microspheres and urchin-like structures (Figure 4a–c). The robust hierarchical nanostructure performs superhydrophobicity (water contact angle reach to 137.1° for porous microspheres and 134.2° for urchin-like structures) (Figure 4a, c), which can be used to fabricate an anti-wetting surface. More interestingly, the interaction between NaDC and RhB can restrict the intramolecular motion and intramolecular charge transfer

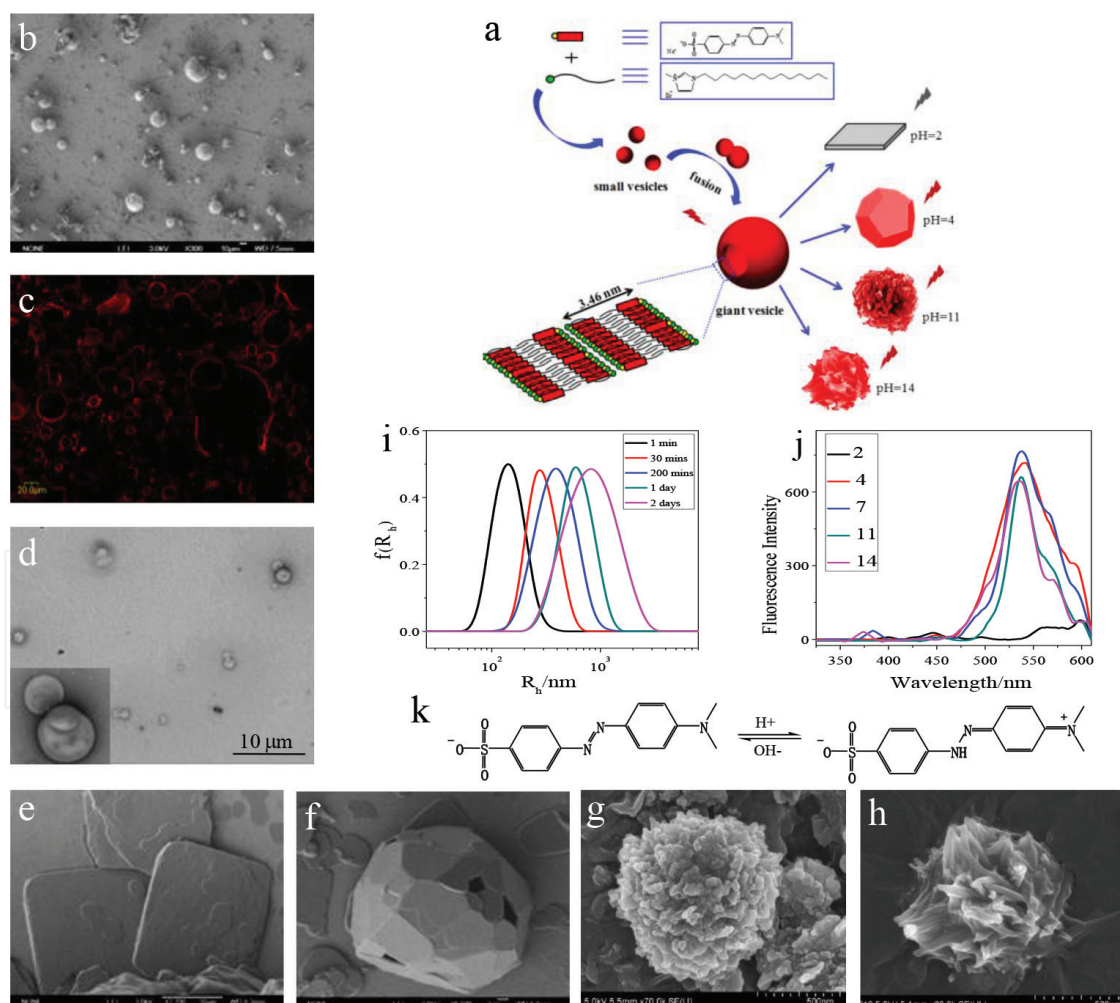


Figure 3. (a) Schematic demonstration of formation of fluorescent giant vesicle and its pH responsiveness. (b) SEM and (c) CLSM image of giant vesicles. (d) TEM images of 0.5 mmol L^{-1} MO/ C_{14} mimBr after 2 days. SEM images of 0.5 mmol L^{-1} MO/ C_{14} mimBr at (e) pH=2, (f) pH=4, (g) pH=11, (h) pH=14. (i) Time-dependant DLS result of 0.5 mmol L^{-1} MO/ C_{14} mimBr. (j) Fluorescence intensity at different pH. (k) pH-dependent mechanism of the MO molecule [26].

state of RhB, minimize aggregation-caused quenching (**Figure 4d, e**), enhance the luminescent efficiency of the dye, and improve the luminescence performance, which open up a new way to build soft materials. Besides, the emitting color of system can also be adjusted by changing the molar ratio of NaDC and RhB (**Figure 4f, g**) and the lifetimes of the precipitates increase greatly with an increase in c_{NaDC} (**Figure 4h**). Moreover, they also used another bile salt sodium cholate (SC) and a cationic dye (MB) to obtain bundles of ultra long nanobelts through ISA approach, and the shape and length of the bundles of SC/MB nanobelts could be easily controlled by changing the SC concentration and the aging temperature. Besides, the bundles of ultra long SC/MB nanobelts exhibited efficient electrocatalytic activity toward ascorbic acid (AA) oxidation in phosphate buffer solution (pH = 7.0). This work provides an alternative way to design and fabricate the ultra long belt-like structures with tunable sizes which may also open up a way for the design and development of optical and electronic devices in the potential bioapplications.

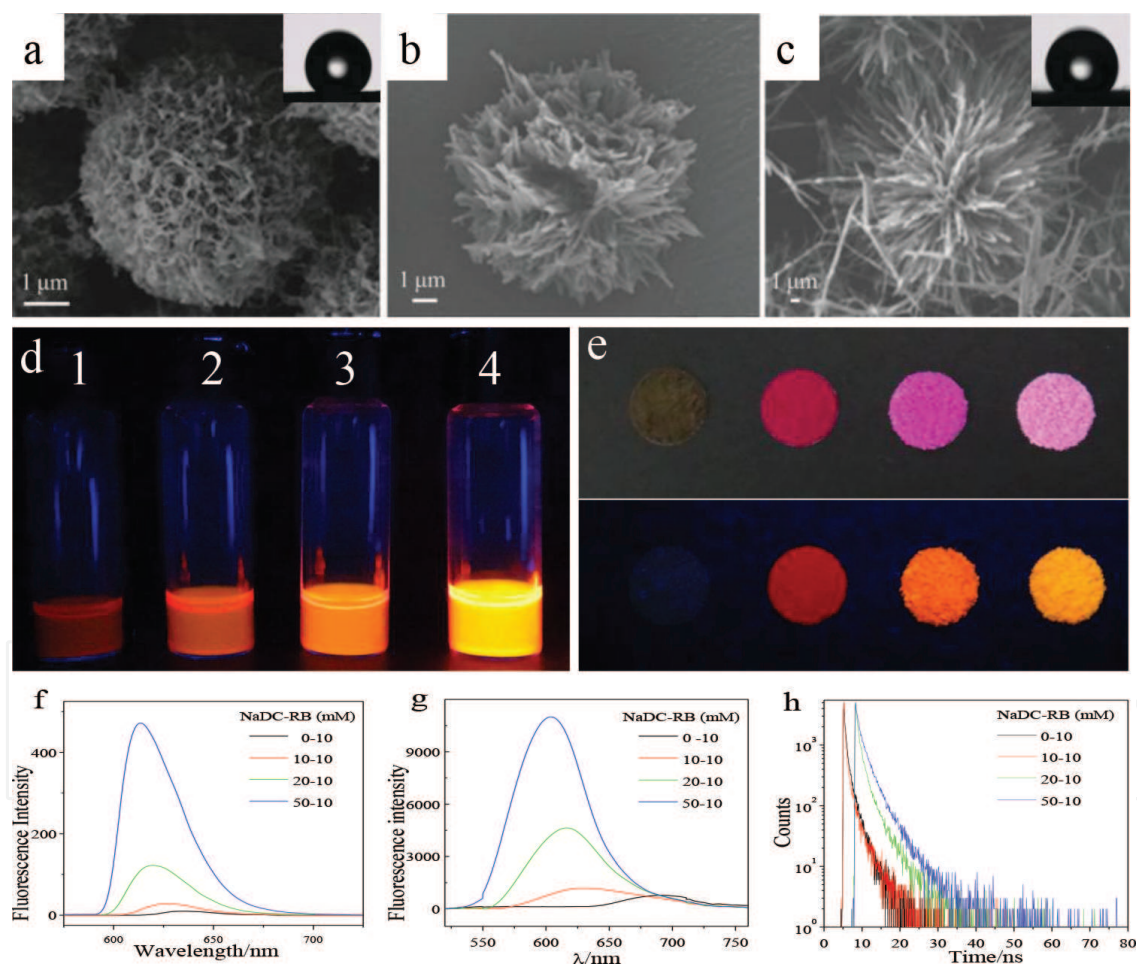


Figure 4. The morphologies of the precipitates of the NaDC/RhB systems when the concentration of RhB was fixed at 10 mmol L^{-1} , while the concentration of NaDC was changed from (a) 10 mmol L^{-1} , (b) 20 mmol L^{-1} , (c) 50 mmol L^{-1} . The inset images of (a) and (c) are the contact angle on the films formed by the sample, respectively. Images of the fluorescence changes in (d): the upper solutions for samples of (1) 10 mmol L^{-1} RhB, (2) 10 mmol L^{-1} NaDC/ 10 mmol L^{-1} RhB, (3) 20 mmol L^{-1} NaDC/ 10 mmol L^{-1} RhB and (4) 50 mmol L^{-1} NaDC/ 10 mmol L^{-1} RhB (excitation at 365 nm), and (e) the powders of the precipitates (upper: under visible light; lower: under UV light, excitation at 365 nm). Changes in the fluorescence spectra of (f) the upper solution and (g) the precipitates obtained for the NaDC/RhB complex samples. (h) Time-resolved fluorescence of the above precipitate samples [33].

Different from conventional planar dyes that always undergo π - π stacking which results in notorious aggregation-caused quenching (ACQ), a new class of dyes with propeller-shaped structure displays aggregation-induced emission (AIE) [34]. However, the drawback of the propeller-shaped topology is that it disfavors self-assembly, so that fluorescent nanostructures based on AIE molecules are still very rarely up to date [35]. In Huang's group, propeller-shaped dye TPE-BPA and surfactant CTAB were chosen to build AIE system [36]. The fluorescence performs the maximum emission at the molar ratio at 1:8 confirming that the optimal interaction between TPE-BPA and CTAB is 1:8 (Figure 5a). And in Cryo-TEM observation, it can be found the formation of vesicles with an average size of 145 nm (Figure 5b). The hydrophilic heads of TPE-BPA molecules are capable of coordinating with metal ions and with the addition of Zn^{2+} to the TPE-BPA@8CTAB system. It can be found that the fluorescence intensity decreases with the addition of Zn^{2+} and research the plateau at a Zn^{2+} /TPE-BPA ratio of 2 (Figure 5d, e), implying that every two coordinating heads share one Zn^{2+} to satisfy the space of an octahedral field. Cryo-TEM reveals the retain of the vesicular structure with smaller size, which was formed by the fission of larger vesicles (Figure 5c). The membranes of cancer cells are highly charged compared to the normal ones, the present results indicate that the high electrical charge may accelerate the cell fission and generate a looser molecular packing and increases the releasing rates of hydrophilic drug DOX (Figure 5f). The report of this research may help to reveal the mystery behind the easy metastasis of the cancer cells and inspire a novel strategy for cancer therapy.

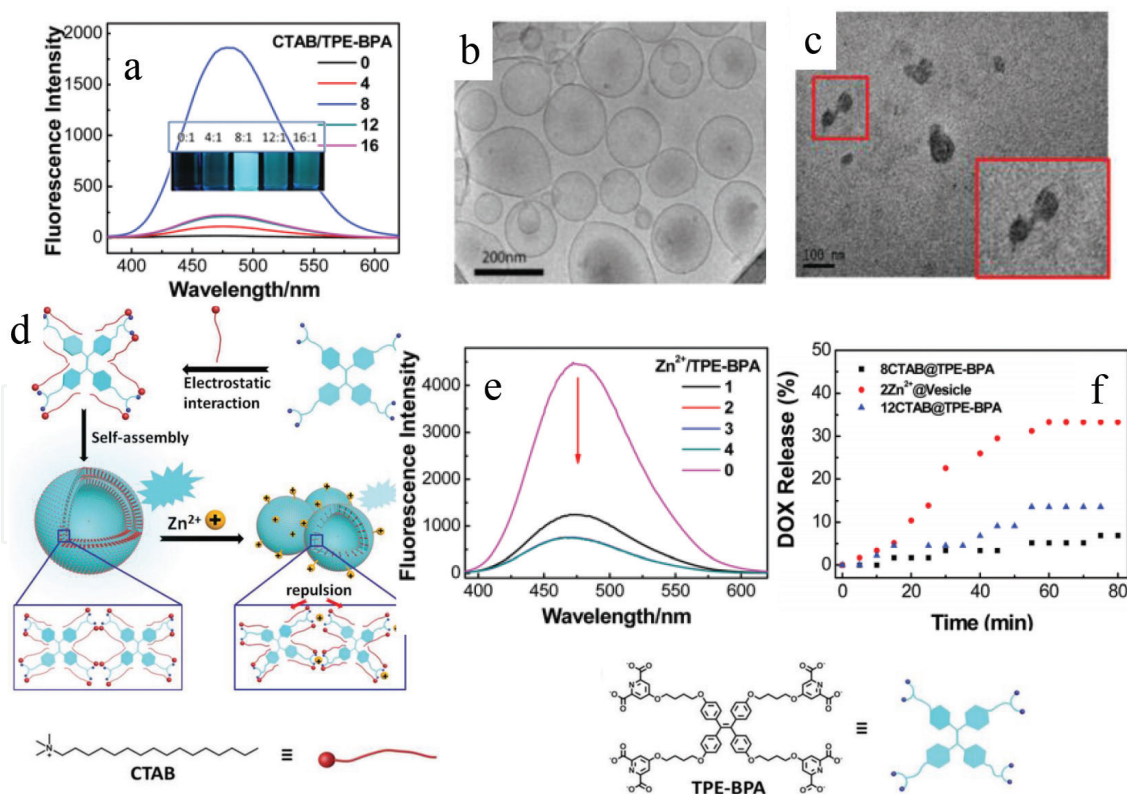


Figure 5. (a) Cryo-TEM image of TPE-BPA@8CTAB vesicle. (b) Fluorescence intensity at different molar ratio of TPE-BPA/CTAB. (c) TEM images of TPE-BPA@8CTAB vesicle triggered by Zn^{2+} . (d) Illustration of self-assembly of TPE-BPA/CTAB vesicles and electrical charge triggered fission of the TPE-BPA/CTAB vesicle. (e) Fluorescence intensity of system with the addition of Zn^{2+} to the TPE-BPA@8CTAB vesicular system. (f) Comparison of the DOX releasing rate in the native TPEBPA@8CTAB vesicle and the charged vesicle of the TPE-BPA@12CTAB, 2 Zn^{2+} @vesicle [35].

3. POM-biomolecule ISA materials

Polyoxometalates (POMs), a large group of metal oxide clusters, represent some of the largest inorganic molecules known so far and have broad applications as catalysts, photoelectronic/magnetic materials, and biologically active materials [37–39]. The POMs are formed by linking metal oxide polyhedra with each other through corner-, edge-, or face-sharing manner, which enable chemists to build POMs with different topologies and sizes. Due to the excess of oxo ligands over metal ions, POMs are usually highly negatively charged, which could interact with positively charged materials by electrostatic interaction. Biomolecule, such as amino acid and polypeptide, is essential for our body [40, 41]. Thus, the self-assembly behavior of POM/biomolecule has potential application in biological field as novel compartments, artificial cell membranes, drug and gene delivery agents [42, 43].

Wu et al. constructed multivalent peptide nanofibers by using short peptides with the synergistic effect of POM clusters [44]. The short peptide L1 adopts a random-coil conformation in aqueous solution, while with the addition of $\text{H}_4\text{SiW}_{12}\text{O}_{40}$ (HSiW), the conformation transition from a random-coil to a β -sheet state (Figure 6a, e). In TEM, one-dimensional (1D) nanofibers were observed after the mixing of L1 with HSiW in water (Figure 6b, c). The multivalent L1/HSiW nanofibers exhibited significantly enhanced antibacterial efficacy, while the inhibitory ability of L1 or HSiW alone was poor (Figure 6d). The assembly nature of POMs enables the enhancement of the antimicrobial efficacy and biological stability of short peptides in situ.

Xin et al. obtained inorganic-organic hybrid vesicles using $\text{POMNa}_9[\text{EuW}_{10}\text{O}_{36}]\cdot 32\text{H}_2\text{O}$ (EuW_{10}) and different amino acids (arginine, lysine, histidine, glutamic acid, aspartic acid, leucine, alanine, and phenylalanine) (Figure 7a, b, g) [45]. The electrostatic interaction between amino

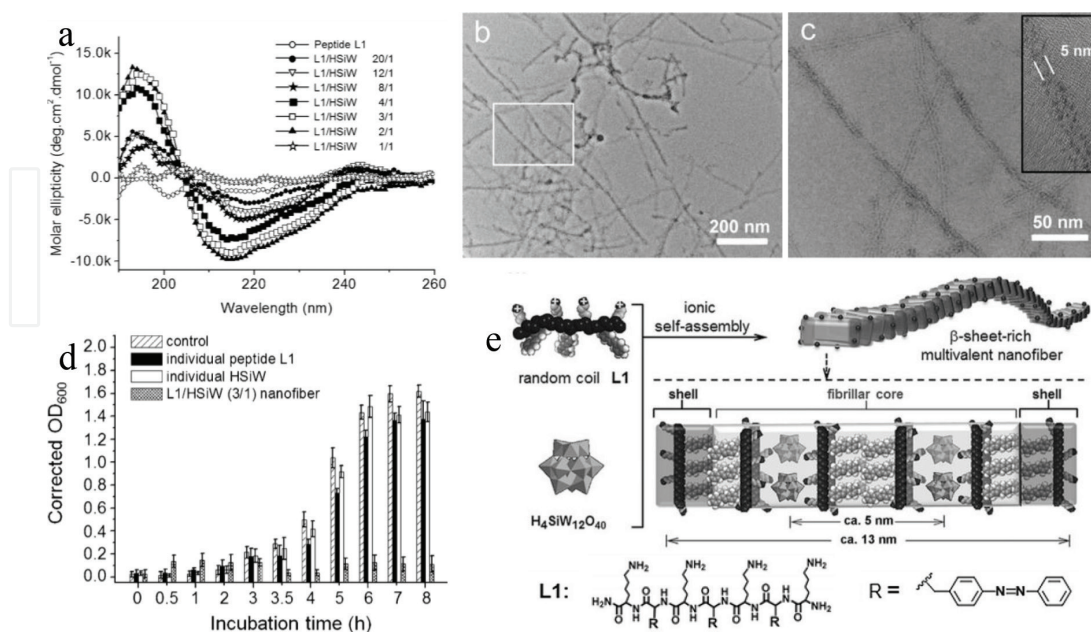


Figure 6. (a) CD spectra of peptide L1 and the L1/HSiW composites at different molar ratios (b, c) TEM image of L1/HSiW at the molar ratio of 3:1. (d) Optical density of *E. coli* with incubation time in the presence of the individual peptide L1, individual HSiW, and L1/HSiW nanofibers. (e) Illustration of self-assembly of L1/HSiW nanofibers [44].

acid and EuW_{10} plays an important role for the formation of vesicle. While the luminescent property is clear distinction among different amino acids that alkaline amino acids (Arg, Lys and His) enhanced the luminescence, acidic amino acids (Glu, Asp) quenched the luminescence and nonpolar amino acids (Leu, Ala, and Phe) have no obviously influence towards luminescence (Figure 7c, d). This is attributed to the strength differences of the electrostatic interactions between amino acids and EuW_{10} cluster. Meaningfully, the Arg/ EuW_{10} fluorescent vesicles can be used to detect Dopamine selectively with the detection limit of $3.2 \mu\text{M}$ on the basis of competition mechanism that dopamine could substitute Arg to form an assembly with EuW_{10} through hydrogen bond interaction between the ammonium group of DA and the oxygen atom of EuW_{10} , leading to fluorescence quenching (Figure 7e, f).

Three-dimensional (3D) hierarchical nanostructures have generated large amounts of interests due to their unique peculiar properties and wide range of potential applications. Among them, nanoflower is a fantastic name of some of the nanomaterials which in microscopic images resemble the flowers. Due to the large surface-to-volume ratio compared with that of bulk materials, nanoflowers have many applications in catalysis, magnetism, nanodevices, sensing

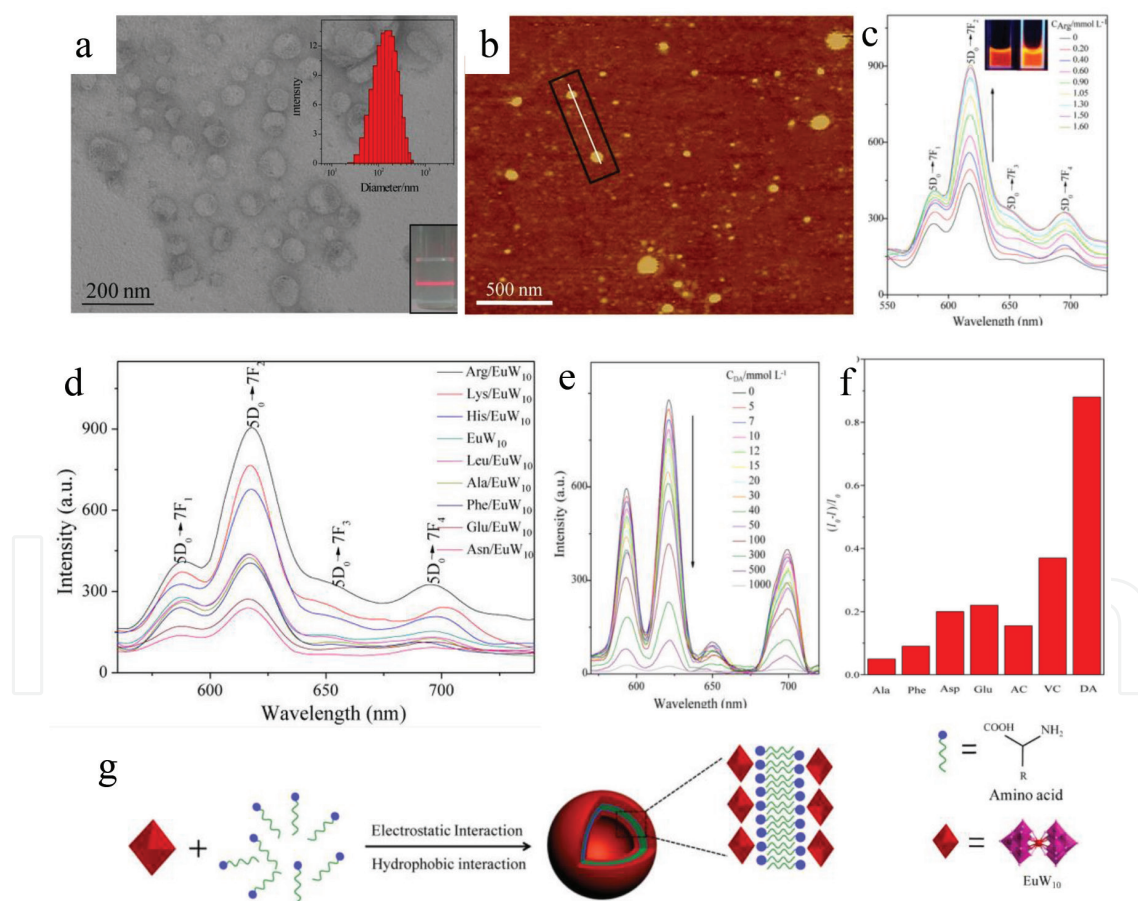


Figure 7. TEM (a) and AFM (b) image of $0.7 \text{ mmol L}^{-1} \text{EuW}_{10}/1.5 \text{ mmol L}^{-1} \text{Arg}$ (insets are the pictures showing the Tyndall effect under the irradiation by a light beam and the hydrodynamic radius of vesicles observed by DLS). (c) Variation of the fluorescence spectra of EuW_{10} (0.7 mmol L^{-1}) upon the titration of Arg. (d) Fluorescence spectra of EuW_{10} incorporated different amino acids. (e) Variation of the fluorescence spectra of $0.7 \text{ mmol L}^{-1} \text{EuW}_{10}/1.5 \text{ mmol L}^{-1} \text{Arg}$ with the addition of DA ($0\text{--}1000 \text{ mmol L}^{-1}$). (f) Fluorescence response of the $\text{EuW}_{10}/\text{Arg}$ system to biological molecules all the concentrations of the biological molecules were 500 mmol L^{-1} . (g) Schematic illustration of the vesicles formed by EuW_{10} and amino acids [45].

and biosensing, and medicine [46–51]. In Xin's group, inorganic-organic hybrid hierarchical nanoflowers structures were prepared by $\text{EuW}_{10}/\text{DA}$ on the basis of ISA strategy with the cooperation of H-bonding interaction (**Figure 8a–c**) [52]. The structure of hybrid can be controlled easily by adjusting the ratio of EuW_{10} and DA, and the formation of $\text{EuW}_{10}/\text{DA}$ hierarchical nanoflowers was monitored by SEM: The protonated DA interact with EuW_{10} by H-bonding and electrostatic interaction, and then, the cores of the flower-like nanostructures were initially formed (**Figure 8d**). Subsequently, more building blocks were stacked into the surface of the cores forming a rough surface and the building blocks aggregated to form the resulted nanoflower (**Figure 8e**). Finally, the hierarchical nanoflowers grew more compact, and the surfaces of the nanopetals became very smooth due to Ostwald ripening in the further growth stage (**Figure 8f**). POMs have been used as catalysts for the oxidation of a variety of compounds such as alkenes, alcohols, sulfides and dyes [53]. In this work, the author calcinated the $\text{EuW}_{10}/\text{DA}$ nanoflower at 350°C for 2 h to get a pure EuW_{10} framework, and the porous EuW_{10} performs excellent degradation ability for MO with the exist of H_2O_2 , the catalyst exhibits only a little loss of photocatalytic activity after six recycles for the degradation of MO, implying that the calcinated porous EuW_{10} can be used as an excellent photocatalyst for multiple cycles to catalyze MO and have potential application for sewage treatment (**Figure 8g–i**). The schematic illustration of the assembly process was shown in **Figure 9**.

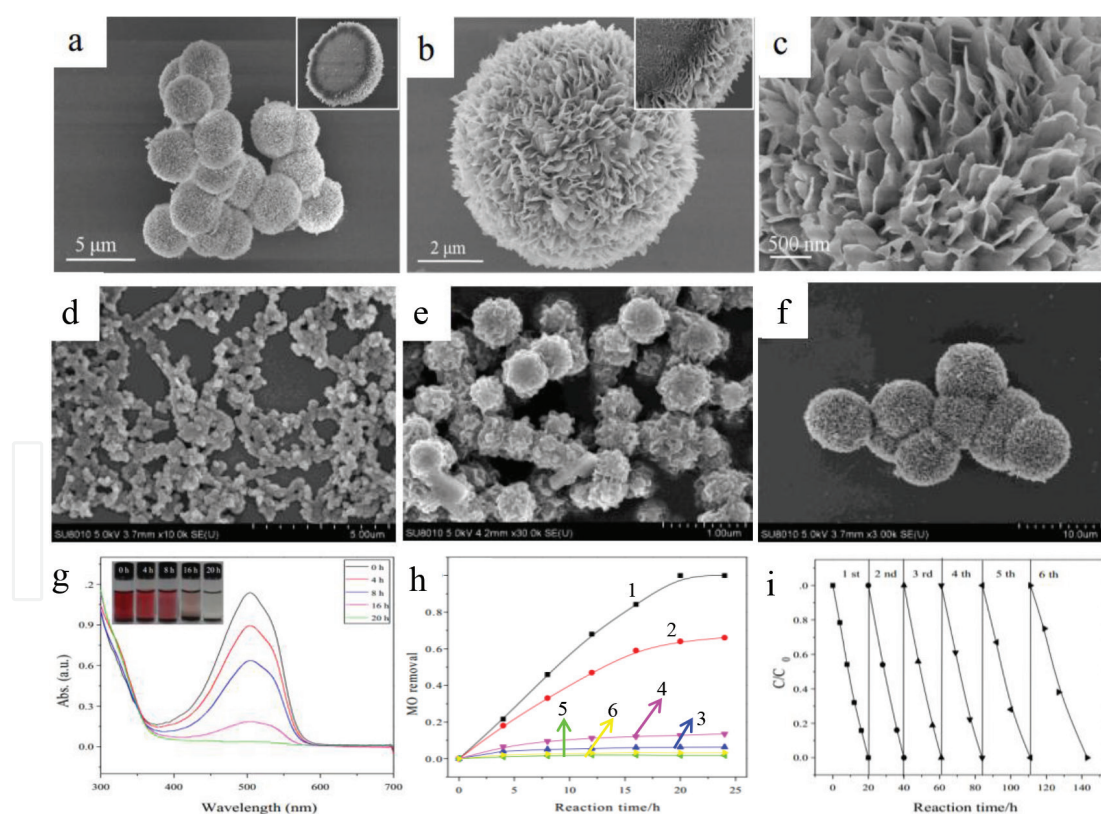


Figure 8. (a, b, c) SEM images of nanoflower formed by $2 \text{ mg mL}^{-1} \text{EuW}_{10}/2 \text{ mg mL}^{-1} \text{DA}$ at different scales. The formation process of EuW_{10} -DA nanoflowers with different incubation time (d) 1 min, (e) 0.5 h, and (f) 2 h. (g) The UV-vis curves of the degradation of MO by calcinated nanoflower. (h) MO degradation over time with different substances: (h-1) calcinated porous $\text{EuW}_{10}/\text{H}_2\text{O}_2$, (h-2) EuW_{10} -DA hybrid nanoflowers/ H_2O_2 , (h-3) $\text{EuW}_{10}/\text{H}_2\text{O}_2$, (h-4) $\text{DA}/\text{H}_2\text{O}_2$, (h-5) H_2O_2 and (h-6) calcinated porous EuW_{10} . (i) The recycling experiment for the degradation of MO using calcinated porous $\text{EuW}_{10}/\text{H}_2\text{O}_2$ system [52].

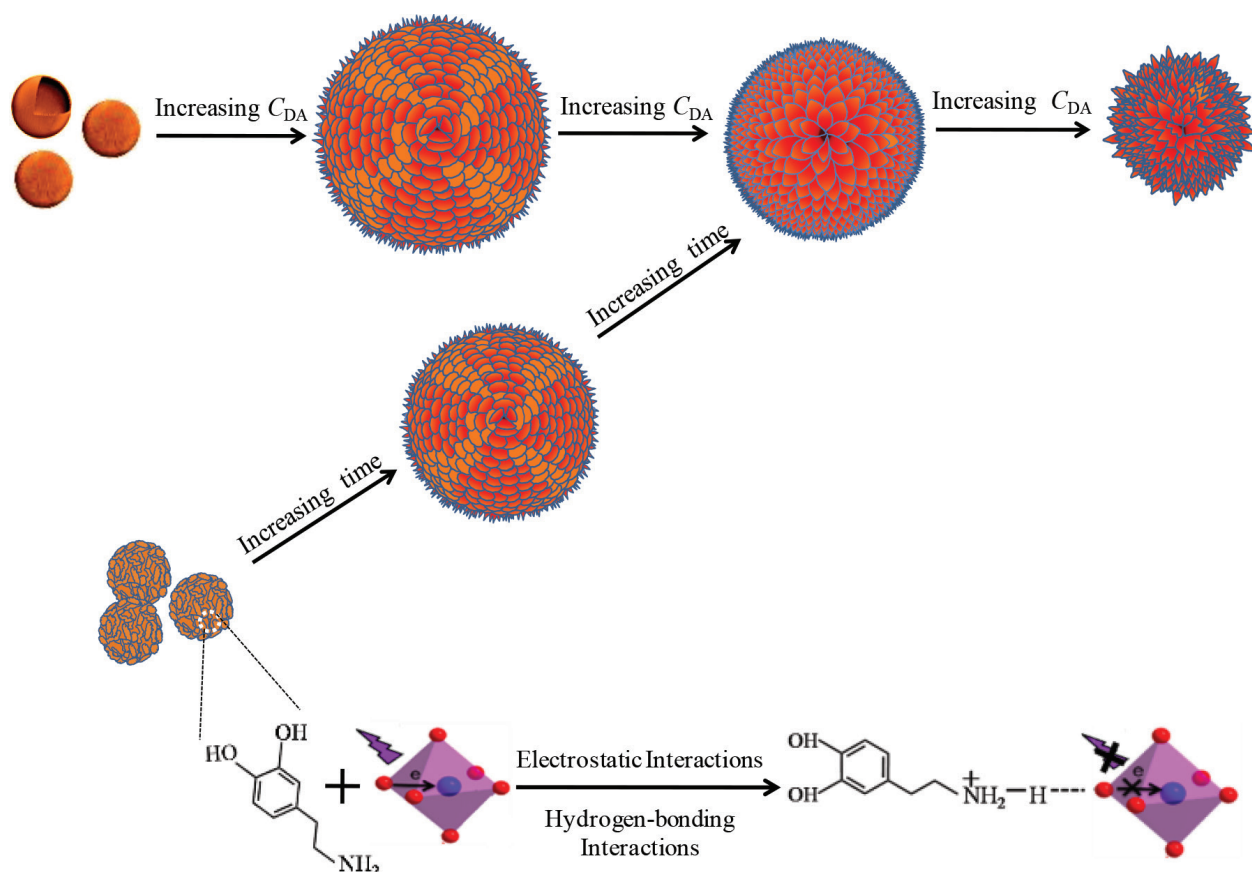


Figure 9. The schematic illustration of the assembly process for EuW₁₀-DA hybrid nanoflowers [52].

4. Conclusion and outlook

In a conclusion, ISA strategy on the basis of electrostatic interaction is a facile and convenient method to prepared complex and hierarchical materials for a wide range of applications without tangle some covalent functionlization. Although many studies have focused on the design and preparation of advanced materials using ISA strategy in the past few years, the successful translation of these laboratory innovations to tackle specific problems in the real world remains a great challenge. It is anticipated that preparing functional materials through ISA strategy is a promising pathway to design and generate new nanoassemblies with unique properties and will certainly play a significant role in the future of material science.

Acknowledgements

We gratefully acknowledge the financial support from the National Natural Science Foundation of China (21573130,21173128) and the Young Scholars Program of Shandong University (2016WLJH20).

Author details

Jinglin Shen¹, Shiling Yuan¹ and Xia Xin^{1,2*}

*Address all correspondence to: xinx@sdu.edu.cn

1 Key Laboratory for Colloid and Interface Chemistry of Education Ministry, School of Chemistry and Chemical Engineering, Shandong University, Jinan, P. R. China

2 National Engineering Technology Research Center for Colloidal Materials, Shandong University, Jinan, P. R. China

References

- [1] Gan Q, Ferrand Y, Bao C, Kauffmann B, Grelard A, Jiang H, Huc I. Helix-rod host-guest complexes with shuttling rates much faster than disassembly. *Science*. 2011; 331: 1172–1175. doi: 10.1126/science.1200143
- [2] Lee C C, Grenier C, Meijer E W, Schenning A P H J. Preparation and characterization of helical self-assembled nanofibers. *Chem. Soc. Rev.* 2009; 38: 671–683. doi: 10.1039/B800407M
- [3] Vera F, Serrano J L, Sierra T. Twists in mesomorphic columnar supramolecular assemblies. *Chem. Soc. Rev.* 2009; 38: 781–796. doi: 10.1039/B800408K
- [4] Huang Z, Kang S K, Banno M, Yamaguchi T, Lee D, Seok C, Yashima E, Lee M, Huang Z, Kang S K, Banno M, Yamaguchi T, Lee D, Seok C, Yashima E, Lee M. Pulsating tubules from noncovalent macrocycles. *Science*. 2012; 337: 1521–1526. doi: 10.1126/science.1224741
- [5] Zhang W, Jin W, Fukushima T, Saeki A, Seki S, Aida T. Supramolecular linear hetero-junction composed of graphite-like semiconducting nanotubular segments. *Science*. 2011; 334: 340–343. doi: 10.1126/science.1210369
- [6] Cordier P, Tournilhac F, Soulie-Ziakovic C, Leibler L. Self-healing and thermoreversible rubber from supramolecular assembly. *Nature*. 2008; 451: 977–980. doi: 10.1038/nature06669
- [7] Aida T, Meijer E W, Stupp S I. Functional supramolecular polymers. *Science*. 2012; 335: 813–817. doi: 10.1126/science.1205962
- [8] Zeng F, Zimmerman S C. Dendrimers in supramolecular chemistry: from molecular recognition to self-assembly. *Chem. Rev.* 1997; 97: 1681–1712. doi: 10.1021/cr9603892
- [9] Chakrabarty R, Mukherjee P S, Stang P J. Supramolecular coordination: self-assembly of finite two- and three-dimensional ensembles. *Chem. Rev.* 2011; 111: 6810–6918. doi: 10.1021/cr200077m

- [10] Yu G, Jie K, Huang F. Supramolecular amphiphiles based on host–guest molecular recognition motifs. *Chem. Rev.* 2015; 115: 7240–7303. doi: 10.1021/cr5005315
- [11] Tan L, Liu Y, Ha W, Ding S, Peng S, Zhang S, Li J. Stimuli-induced gel–sol transition of multi-sensitive supramolecular β -cyclodextrin grafted alginate/ferrocene modified pluronic hydrogel. *Soft Matter*, 2012; 8: 5746–5749. doi: 10.1039/C2SM25084E
- [12] Zhu Y, Liu L, Du J. Probing into homopolymer self-assembly: how does hydrogen bonding influence morphology? *Macromolecules*, 2013; 46: 194–203. doi: 10.1021/ma302176a
- [13] Tahara K, Lei S B, Adisojoso J, Feyter S De, Tobe Y. Supramolecular surface-confined architectures created by self-assembly of triangular phenylene–ethynylene macrocycles via van der Waals interaction. *Chem. Commun.* 2010; 46: 8507–8525. doi: 10.1039/C0CC02780D
- [14] Zhu Y, Fan L, Yang B, Du J. Multifunctional homopolymer vesicles for facile immobilization of gold nanoparticles and effective water remediation. *ACS Nano*. 2014; 8: 5022–5031. doi: 10.1021/nn5010974
- [15] Li Q, Chen X, Wang X, Zhao Y. Ionic self-assembled wormlike nanowires and their cyclodextrin inclusion-tuned transition. *J. Phys. Chem. B*, 2010; 114: 10384–10390. doi: 10.1021/jp104801m
- [16] Liu T, Tian W, Zhu Y. How does a tiny terminal alkynyl end group drive fully hydrophilic homopolymers to self-assemble into multicompart ment vesicles and flower-like complex particles? *Polym. Chem.* 2014; 5: 5077–5088. doi: 10.1039/C4PY00501E
- [17] Faul C F J, Antonietti M. Ionic self-assembly: facile synthesis of supramolecular materials. *Adv. Mater.* 2003; 15: 673–683. doi: 10.1002/adma.200300379
- [18] Thool G S, Narayanaswamy K, Venkateswararao A, Naqvi S, Gupta V, Chand S, Vivekananthan V, Koner RR, Krishnan V, Singh SP. Highly directional 1D-supramolecular assembly of new diketopyrrolopyrrole based gel for organic solar cell applications. *Langmuir*. 2016; 32: 4346–4351. doi: 10.1021/acs.langmuir.6b00846
- [19] Faul C F J. Ionic self-assembly for functional hierarchical nanostructured materials. *Acc. Chem. Res.* 2014; 47: 3428–3438. doi: 10.1021/ar500162a
- [20] Adak S, Datta S, Bhattacharya S, Banerjee R. Imidazolium based ionic liquid type surfactant improves activity and thermal stability of lipase of *Rhizopus oryzae*. *J. Mol. Catal. B: Enzym.* 2015; 119: 12–17. doi: 10.1016/j.molcatb.2015.05.010
- [21] Wang B, Song A, Feng L, Ruan H, Li H, Dong S, Hao J. Tunable amphiphilicity and multifunctional applications of ionic liquid-modified carbon quantum dots. *ACS Appl. Mater. Interfaces* 2015; 7: 6919–6925. doi: 10.1021/acsami.5b00758
- [22] Guan Y, Zakrevskyy Y, Stumpe J, Antonietti M, Faul C F. Perylene diimide-surfactant complexes: thermotropic liquid-crystalline materials via ionic self-assembly. *Chem. Commun.* 2003; 7: 894–895. doi: 10.1039/B211753C

- [23] Zhao M, Zhao Y, Zheng L, Dai C. Construction of supramolecular self-assembled microfibers with fluorescent properties through a modified ionic self-assembly (ISA) strategy. *Chem. Eur. J.* 2013; 19: 1076–1081. doi: 10.1002/chem.201203062
- [24] Faul C F J, Antonietti M. Facile synthesis of optically functional, highly organized nanostructures: dye–surfactant complexes. *Chem. Eur. J.* 2002; 8: 2764–2768. doi: 10.1002/1521-3765(20020617)8:12<2764::AID-CHEM2764>3.0.CO;2-X
- [25] Shen J, Xin X, Liu T. Ionic self-assembly of a giant vesicle as a smart microcarrier and microreactor. *Langmuir.* 2016; 32: 9548–9556. doi: 10.1021/acs.langmuir.6b01829
- [26] Shen J, Xin X, Liu G. Fabrication of smart pH-responsive fluorescent solid-like giant vesicles by ionic self-assembly strategy. *J. Phys. Chem. C.* 2016; 120: 27533–27540. doi: 10.1021/acs.jpcc.6b08140
- [27] Fan Y, Zhang D, Wang J, Jin H, Zhou Y, Yan D. Preparation of anion-exchangeable polymer vesicles through the selfassembly of hyperbranched polymeric ionic liquids. *Chem. Commun.* 2015; 51: 7234–7237. doi: 10.1039/C5CC01802A
- [28] Galantini L, Gregorio M C, Gubitosi M, Travaglini L, Tato J V, Jover A, Meijide F, Tellini V H S, Pavel N V. Bile salts and derivatives: rigid unconventional amphiphiles as dispersants, carriers and superstructure building blocks. *Curr. Opin. Colloid Interface Sci.*, 2015; 20: 170–182. doi: 10.1016/j.cocis.2015.08.004
- [29] Schefer L, Sánchez-Ferrer A, Adamcik J, Mezzenga R. Resolving self-assembly of bile acids at the molecular length scale. *Langmuir*, 2012; 28: 5999–6005. doi: 10.1021/la300384u
- [30] Tung S H, Huang Y E, Raghavan S R. A new reverse wormlike micellar system: mixtures of bile salt and lecithin in organic liquids. *J. Am. Chem. Soc.* 2006; 128: 5751–5756. doi: 10.1021/ja0583766
- [31] Sun X, Xin X, Tang N, Guo L, Wang L, Xu G. Manipulation of the gel behavior of biological surfactant sodium deoxycholate by amino acids. *J. Phys. Chem. B.* 2014; 118: 824–832. doi: 10.1021/jp409626s
- [32] Reschly E J, Ai N, Ekins S, Welsh W J, Hagey L R, Hofmann A F, Krasowski M D. Evolution of the bile salt nuclear receptor FXR in vertebrates, *J. Lipid Res.* 2008; 49: 1577–1587. doi: 10.1194/jlr.M800138-JLR200
- [33] Song Z, Xin X, Shen J. Reversible controlled morphologies switching between porous microspheres and urchin-like microcrystals for NaDC/RhB self-assembly and their multifunctional applications. *J. Mater. Chem. C.* 2016; 4: 8439–8447. doi: 10.1039/C6TC02329K
- [34] Hong Y, Lam J W Y, Tang B Z. Aggregation-induced emission. *Chem. Soc. Rev.* 2011; 40: 5361–5388. doi: 10.1039/C1CS15113D
- [35] Li J, Liu K, Han Y, Tang B, Huang J, Yan Y. Fabrication of propeller-shaped supra-amphiphile for construction of enzyme-responsive fluorescent vesicles. *ACS Appl. Mater. Interfaces.* 2016; 8: 27987–27995. doi: 10.1021/acsami.6b08620

- [36] Li J, Shi K, Drechsler M, Tang B, Huang J, Yan Y. A supramolecular fluorescent vesicle based on a coordinating aggregation induced emission amphiphile: insight into the role of electrical charge in cancer cell division. *Chem. Commun.* 2016; 52: 12466–12469. doi: 10.1039/C6CC06432A
- [37] Hill C L. Introduction: polyoxometalates multicomponent molecular vehicles to probe fundamental issues and practical problems. *Chem. Rev.* 1998; 98: 1–2. doi: 10.1021/cr960395y
- [38] Long D L, Burkholder E, Cronin L. Polyoxometalate clusters, nanostructures and materials: from self assembly to designer materials and devices. *Chem. Soc. Rev.* 2007; 36: 105–121. doi: 10.1039/B502666K
- [39] Yin P, Li D, Liu T. Solution behaviors and self-assembly of polyoxometalates as models of macroions and amphiphilic polyoxometalate–organic hybrids as novel surfactants. *Chem. Soc. Rev.* 2012; 41: 7368–7383. doi: 10.1039/C2CS35176E
- [40] Shimizu T, Masuda M, Minamikawa H. Supramolecular nanotube architectures based on amphiphilic molecules. *Chem. Rev.* 2005; 105: 1401–1443. doi: 10.1021/cr030072j
- [41] Landsmann S, Luka M, Polarz S. Bolaform surfactants with polyoxometalate head groups and their assembly into ultra-small monolayer membrane vesicles. *Nat. Commun.* 2012; 3: 1299. doi: 10.1038/ncomms2321
- [42] Stanish I, Lowy D A, Hung C W, Singh A. Vesicle-based rechargeable batteries. *Adv. Mater.* 2005; 17: 1194–98. doi: 10.1002/adma.200401132
- [43] Duan Q, Cao Y, Li Y, Hu X, Xiao T, Lin C. pH responsive supramolecular vesicles based on water-soluble pillar[6]-arene and ferrocene derivative for drug delivery. *J. Am. Chem. Soc.* 2013; 135: 10542–10549. doi: 10.1021/ja405014r
- [44] Li J, Chen Z, Zhou M. Polyoxometalate-driven self-assembly of short peptides into multivalent nanofibers with enhanced antibacterial activity. *Angew. Chem. Int. Ed.* 2016; 128: 2638–2641. doi: 10.1002/ange.201511276
- [45] Zhang H, Guo L, Xie Z. Tunable aggregation-induced emission of polyoxometalates via amino acid-directed self-assembly and their application in detecting dopamine. *Langmuir.* 2016; 32: 13736–13745. doi: 10.1021/acs.langmuir.6b03709
- [46] Zeng M, Li Y, Liu F, Yang Y, Mao M, Zhao X. Cu doped OL-1 nanoflower: a UV-vis-infrared light-driven catalyst for gas-phase environmental purification with very high efficiency. *Appl. Catal. B: Environ.* 2017; 200: 521–529. doi: 10.1016/j.apcatb.2016.07.042
- [47] Huang K, Liu Y, Wang L. Molybdenum disulfide nanoflower-chitosan-Au nanoparticles composites based electrochemical sensing platform for bisphenol A determination. *J. Hazard. Mater.* 2014; 276: 207–215. doi: 10.1016/j.jhazmat.2014.05.037
- [48] He S, Hu C, Hou H, Chen W. Ultrathin MnO₂ nanosheets supported on cellulose based carbon papers for high-power supercapacitors. *J. Power. Sources.* 2014; 246: 754–761. doi: 10.1016/j.jpowsour.2013.08.038

- [49] Wang D, Pan Z, Wu Z, Wang Z, Liu Z. Hydrothermal synthesis of MoS₂ nanoflowers as highly efficient hydrogen evolution reaction catalysts. *J. Power Sources*. 2014; 264: 229–234. doi: 10.1016/j.jpowsour.2014.04.066
- [50] Liu Y, Jiao Y, Zhang Z, Qu F, Umar A, Wu X. Hierarchical SnO₂ nanostructures made of intermingled ultrathin nanosheets for environmental remediation, smart gas sensor, and supercapacitor applications. *ACS Appl. Mater. Interfaces*. 2014; 6: 2174–2184. doi: 10.1021/am405301v
- [51] Hu L, Ren Y, Yang H, Xu Q. Fabrication of 3D hierarchical MoS₂/polyaniline and MoS₂/C architectures for lithium-ion battery applications. *ACS Appl. Mater. Interfaces*. 2014; 6: 14644–14652. doi: 10.1021/am503995s
- [52] Zhang H, Guo L Y, Jiao J. Ionic Self-assembly of Polyoxometalate-Dopamine Hybrid Nanoflowers with Excellent Catalytic Activity for Dyes. *ACS Sustainable Chem. Eng.* 2017; 5: 1358–1367. DOI: 10.1021/acssuschemeng.6b01805
- [53] Mizuno N, Yamaguchi K, Kamata K. Epoxidation of olefins with hydrogen peroxide catalyzed by polyoxometalates. *Coord. Chem. Rev.* 2005; 249: 1944–1956. DOI:10.1016/j.ccr.2004.11.019

IntechOpen